ELSEVIER

Journal of Power Sources 65 (1997) 173–178

JOURNAL OF POWER SOURCES

26

Dynamic interaction of a proton exchange membrane fuel cell and a lead–acid battery

John C. Amphlett *, Erick H. de Oliveira, Ronald F. Mann, Pierre R. Roberge, Aida Rodrigues, John P. Salvador

Department of Chemistry and Chemical Engineering, Royal Military College of Canada, Kingston, Ont., K7K 5L0, Canada

Received 4 November 1996; accepted 29 November 1996

Abstract

An air-independent fuel cell/lead–acid battery power system could extend the submerged endurance of conventional submarines. This load sharing system requires a deep understanding of how the systems will interact, both from an operational perspective and to avoid high battery voltages that may result in excessive hydrogen production in a completely contained environment. A methodology for predicting the response of the coupled systems was developed to predict the transient behaviour under various loads at standard operating conditions.

Keywords: Fuel cells; Proton exchange membrane; Lead–acid batteries; Applications/submarines

1. Introduction

For a wide number of transport applications, fuel cells are seen as providing a highly efficient, non-polluting, means of electrical power generation. Because reactants may be stored on-board, the application holds significant promise for underwater platforms in general, and naval submersibles and submarines in particular.

The submarine is a covert asset whose primary advantage is its ability to remain undetected underwater; however, the conventional submarine must surface every few days in order to snorkel air for running diesel generators, which are used to recharge the batteries. This is an indiscretion which makes the submarine vulnerable to detection. An air-independent fuel cell system would potentially allow the submarine to remain submerged for up to three weeks.

While a submarine was operating under fuel cell power, various conditions would connect the fuel cells and battery banks together for intervals of varying duration. For example, while submerged, the fuel cell might operate independently for long periods of time, while supplying a trickle charge to the battery bank. Such periods of coupled operation raise the question of the dynamic behaviour of the paralleled fuel cell/battery system. It is conceivable, for example, that while running on the surface during a following sea, the propeller might leave the water briefly. This would represent a sudden load shed, and cause the fuel cell to temporarily discharge excess current into the batteries. Similarly, the option exists to take advantage of uneventful transits by running the fuel cell at maximum power in order to charge the battery bank. Although this scenario represents an inefficient use of hydrogen reserves (due to the limited charging efficiency of the battery), it serves to demonstrate the importance of an understanding of the interaction between the battery and the fuel cell stack.

Fuel cells and lead–acid batteries exhibit different electrical behaviour. If they are to be connected, it is important to have a fundamental understanding of their independent characteristics, before paralleling them together. This is of particular significance considering the extremely large capacitance of the lead–acid battery — the system must be designed to never operate in such a way that the battery attempts to drive current into the fuel cell.

A methodology for predicting the response of a coupled fuel cell and battery system was developed to predict the system behaviour under various loads under standard operating conditions. A model for the system based on the bench-scale apparatus was then applied to a proposed fuel cell/battery system for submarine propulsion.

2. Theory

PEM fuel cells and lead–acid batteries are both electrochemical power sources in which reactants are consumed in

* Corresponding author.

PII S0378-7753(97)02472-5

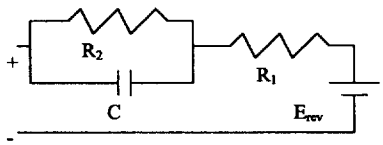

Fig. 1. Electrical circuit representing the response of a lead–acid battery at low current densities.

the direct production of electricity. The fundamental difference between the systems is that battery electrodes contain all of their energy reserves, whereas fuel cell reactants are stored external to the system and are pumped into the electrodes.

Most lead–acid batteries on submarines are flooded cells, which are constructed by placing a negative lead electrode and a positive lead dioxide electrode in a sulfuric acid bath. The negative lead electrode is constructed as a flat plate, while the positive lead dioxide electrode is either a flat pasted plate or of tubular positive construction. Since the electrodes are porous, they have a relatively large surface area.

Although a number of mechanistic and complex empirical models of a lead–acid battery have been developed, most models focus on describing the steady state behaviour. As it was intended to focus on only the dynamic behaviour of the systems, it was decided to model the lead–acid battery using a circuit element representation.

Fig. 1 shows the principle elements describing the short term lead–acid battery behaviour at low current densities (at high current densities, there is a further impedance that must be included). E_{rev} is the open-circuit voltage (V) of the cell, while R_1 represents the ohmic resistance (ohms) in the electrolyte and the current collectors. R_2 represents the overvoltage (ohms) due to diffusion, migration and charge transfer. C represents the combined double layer capacitance (farads) of the electrodes, which is extremely large due to the large surface area.

This type of model will show how the voltage will behave in response to a load or a charging current; unfortunately, all of the parameters are strong functions of the system states [1,2]. For example, E_{rev} is a direct function of the acid concentration and temperature, and the resistance terms will be different depending upon the state-of-charge (SOC), temperature, current density, and whether or not the battery is charging or being discharged. For the study, estimates of the parameters were obtained by holding all parameters constant except the SOC and the current.

A proton exchange membrane (PEM) fuel cell combines hydrogen and oxygen gas over a platinum catalyst to produce electrical power, as well as heat and liquid water by-products. The solid polymer membrane containing the catalyst replaces the liquid electrolyte normally found in batteries and some other types of fuel cells.

Precise semi-mechanistic models describing fuel cell behaviour have been developed previously; however, most of the models focus on steady state behaviour [3–5]. Preliminary dynamic fuel cell models have been developed but only account for the thermal dynamic effects as the cell voltage response was taken as a steady-state measurement based on the operating conditions at a certain point in time. These models assumed that the thermal dynamics were far slower than the electrochemical dynamic behaviour for the time steps required for that study. The time steps were on the magnitude of minutes. It was therefore decided to also create a circuit element model of a fuel cell stack. Although experience indicated that the fuel cell had a very fast time constant, it was decided to use the same electric circuit that was used for the battery (Fig. 1) to ensure that information was not being left out.

In the Canadian AIP scenario, a 224 cell lead–acid battery would be paralleled with a 400 kW fuel cell system [6] consisting of thousands of individual fuel cells connected in a series/parallel combination. Since a single submarine lead–acid cell normally operates in the 200–8000 A range, and all of the fuel cell stacks available at RMC for testing had the cells connected in series, it was decided to perform the present work with smaller batteries. Otherwise, the flow of current to or from the battery would have been too small to act as representative of the battery behaviour. Tests were performed on Varta 240 Ah tubular positive stationary cells, which were approximately 1/35 scale of the Varta cells currently in use on Canadian vessels. Earlier work had indicated that under low to moderate current densities, both systems responded similarly during cycling and in response to load changes.

3. Experimental

Testing proceeded in three parts. First, estimates of the circuit elements for the battery had to be obtained. An experimental design was produced in which SOC, current density, and direction of current flow were varied while all of the other state variables were held constant. Healthy lead–acid cells that had experienced less than 30 cycles were used, and their temperature was maintained at 22°C ($\pm$ 1°C) throughout the testing.

The battery, consisting of two cells in series, was then connected to a fast switching constant current electronic load and a constant current power supply. It was cycled at a $C/5$ rate. To obtain parameter estimates, it would be discharged to a desired SOC, and left to sit overnight to allow acid gradients within the cells to dissipate. At this point, either a constant current load or a constant current source was connected to the cells, and the circuit was maintained until the voltage reached steady state. Cells were discharged at 50% and 80% SOC (normal operating range) at $C/97$ and $C/23$ rates (corresponding to the initial power rates that would likely be required on a submarine). All of the charging steps were performed between 50% and 100% SOC at current densities ranging from $C/12$ to $C/60$, the maximum current being chosen to coincide with the highest current likely available from a fuel cell system in an AIP configuration. However, some of the charging steps were performed only a few

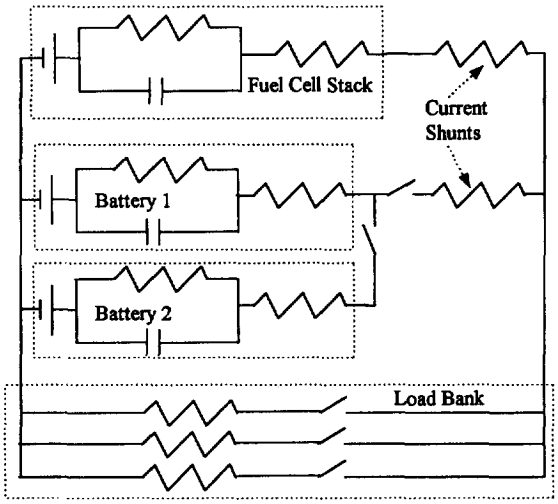

Fig. 2. Electrical circuit representing the coupled system, with two battery banks included.

hours after resting to observe the effect of not starting at steady state on the system.

To obtain estimates of the battery parameters, the total battery resistance (R_1+R_2) was obtained from the steady state data after a current step had been performed. Individual estimates of the parameters were then obtained by performing a least-squares analysis on the data with the derived solution to the electric circuit. This was repeated for each step response. A similar process was used to obtain the fuel cell parameters from the data.

The second part of the testing involved determining the parameters of the fuel cell system. Although stack temperature, current density, and inlet pressure of fuel and oxidant all influence the stack voltage, for the purposes of this study, everything was held constant except the current density. A five-cell fuel cell stack was then connected to a purely resistive load bank. Since in normal operation the fuel cell system would be operated at steady state, with step changes occurring as required, it was decided to perform step changes from a 75 A baseline. Steps of varying size were performed in both directions to determine the degree of linearity of the system. The fuel cell stack was maintained at 70°C (± 1°C) throughout the tests with pure hydrogen and air (21% oxygen) at pressures of 307 kPa each. The stoichiometry was maintained at 2.0/2.0 stoichiometry for hydrogen and air.

Fuel cell and battery currents were measured using shunts, while the high frequency voltage data were collected using an IOTech ADC 488/8SA analog to digital converter at a rate of 1000 measurements per channel per second.

The third part of the testing involved connecting a two-cell battery and a five-cell fuel cell stack together in parallel with a resistive load bank. The number of cells was chosen such that the voltages would be compatible, with the open-circuit fuel cell voltage higher than the battery voltage. To evaluate the effect of different battery/fuel cell combinations, the two cell battery (identified as battery 1 in Fig. 2) was paralleled with a second two cell lead–acid battery (battery 2) and the testing repeated.

A four step test programme was used. First, battery 1 was switched into the system while the fuel cell was under load. The load had been chosen such that the bus voltage would be only slightly higher than the battery voltage. After the system stabilised, step two removed the load from the system. Steps 3 and 4 involved the addition of considerably larger loads (0.11 ohm) to the system. The experimental results were then compared with the predicted voltage and current response generated using estimates of the parameters from the first two parts of the testing. The entire procedure was then repeated with both batteries 1 and 2 switched into the circuit.

4. Results and discussion

4.1. Battery

The battery voltage exhibited a first-order response to both the imposition of a constant current load and the onset of constant current charging. Furthermore, the circuit model parameters were all strong functions of the battery state. The response to a load change indicated that R_1 was relatively constant, while R_2 decreased with increasing current, as shown in Table 1. The capacitance term, C, appeared to be more dependent on the state of charge than the current density, ultimately resulting in a smaller time constant at higher current densities and lower states of charge. This corresponds with other work in the area [1], which suggested that the parameters were all non-linear functions of the battery state.

When a constant current charging step was imposed on the battery, similar behaviour was demonstrated, although the parameters had shifted. R_1 was relatively constant, but R_2 increased dramatically as the battery's state-of-charge increased beyond 80%. R_2 still decreased as the current density increased. Fairly strong fits of the data were often, although not always, available, as demonstrated in Fig. 3. The difference between the experimental voltage and the true voltage was usually less than 20 mV at the worst point, and often less than 10 mV. However, once the conditions dictated that the battery would be gassing aggressively, such as beyond 2.35 V per cell at steady state, the model was incapable of adequately describing the response.

A further source of error developed whenever the battery had not been allowed to sit at open-circuit for a sufficient length of time before the next charging step. If the open-

Table 1
Battery parameters at various SOC and discharge rates

SOC	Current rating	R_1 (ohms)	R_2 (ohms)	C (farads)	Time constant (s)
80%	C/97	0.0032	0.012	12800	156
80%	C/23	0.0036	0.0052	12500	65
50%	C/95	0.0030	0.014	6500	88
50%	C/24	0.0028	0.0046	5000	23

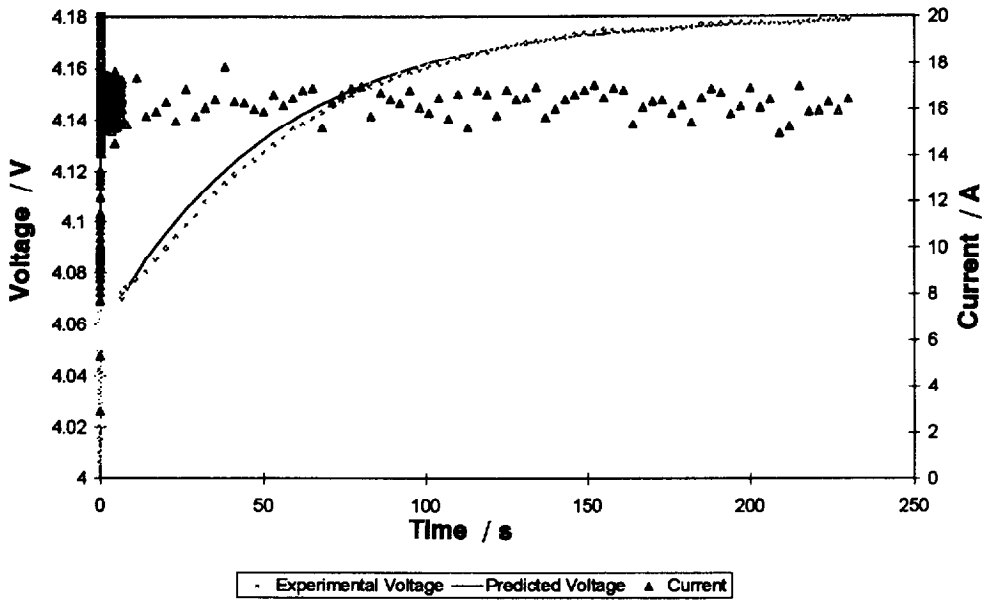

Fig. 3. Comparison of predicted battery voltage to experimental voltage in response to a charging current of 15 A.

circuit voltage had not fully returned to steady state, R_2 estimates would be slightly low. Furthermore, due to the extremely high correlation between R_2 and C, small errors in one parameter would have a significant impact on the other.

4.2. Fuel cell

At constant stoichiometry and temperature, the steady state fuel cell response to load changes was very linear at all but the lowest current densities below 15 A, as shown in Fig. 4. From this, the steady state fuel cell response could be simplified to:

$$\text{Stack voltage} = 4.502 - 0.0121I$$

The transient behaviour was also linear, and exhibited two notable characteristics. First, there was an extremely fast time constant of approximately 3 ms (± 2 ms), with the voltage reaching steady state within 10 to 15 ms. Due to the very small fuel cell capacitance, it would often be difficult to fully differentiate the capacitance from effects due to switching transients. The second notable effect was a recovery of the cell voltage in the direction opposite to the initial transient movement. This longer term response occurred over 2 to 10 s, and represented a change in stack voltage of less than 15 mV. It did not appear to be correlated with the size or direction of the load change. These effects can be noted in Fig. 5.

4.3. Parallel operation of the battery and fuel cell

Once the battery and the fuel cell were placed on the same bus, the fuel cell voltage quickly moved to match the battery voltage, exhibiting a time constant of approximately 6 ms. The fuel cell voltage moved much further than the battery voltage due to its larger internal resistance. As charging continued, the rising battery voltage caused the current flowing from the fuel cell to decrease, ultimately resulting in a steady

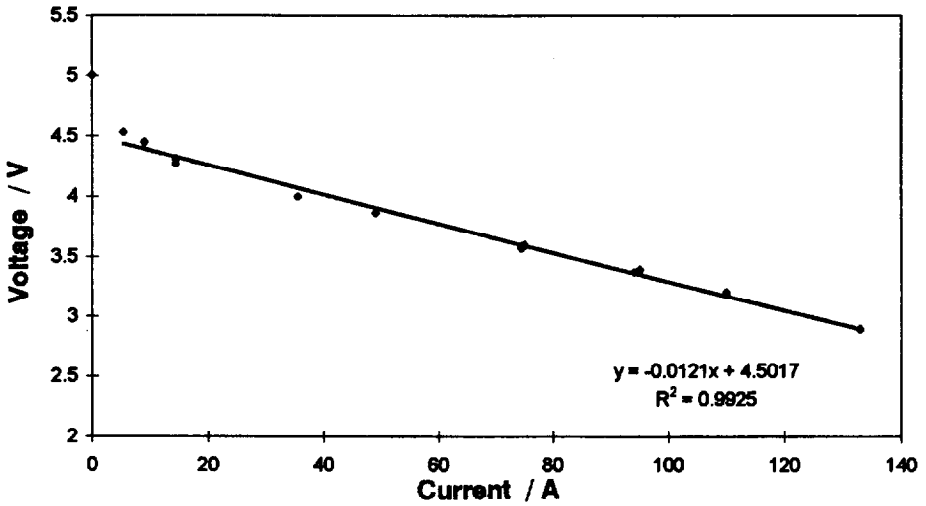

Fig. 4. Fuel cell voltage (V), as a function of current, using hydrogen/air at 2.0/2.0 stochiometry, 307/307 kPa and $T_{stack} = +70°C$.

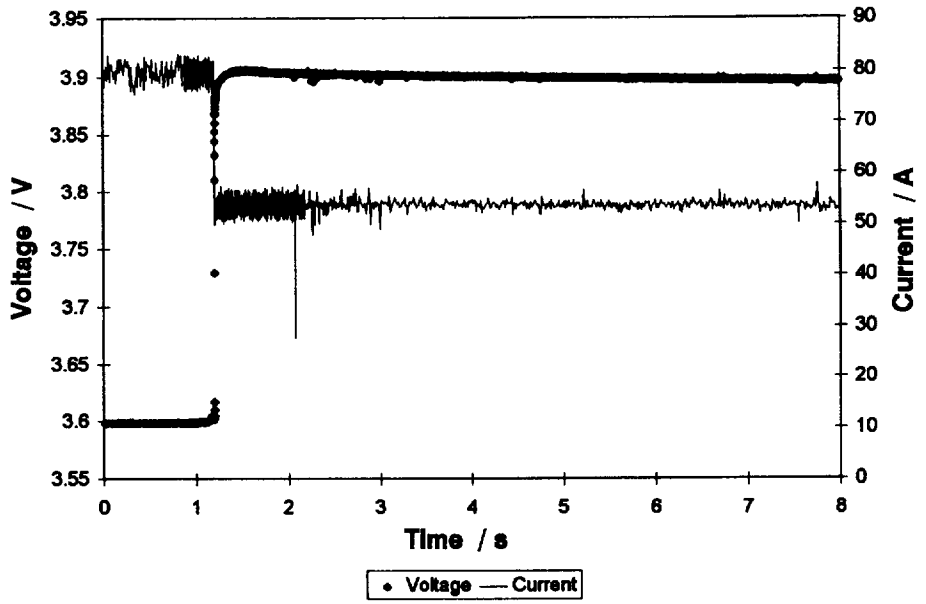

Fig. 5. Response of fuel cell voltage to a reduction in load.

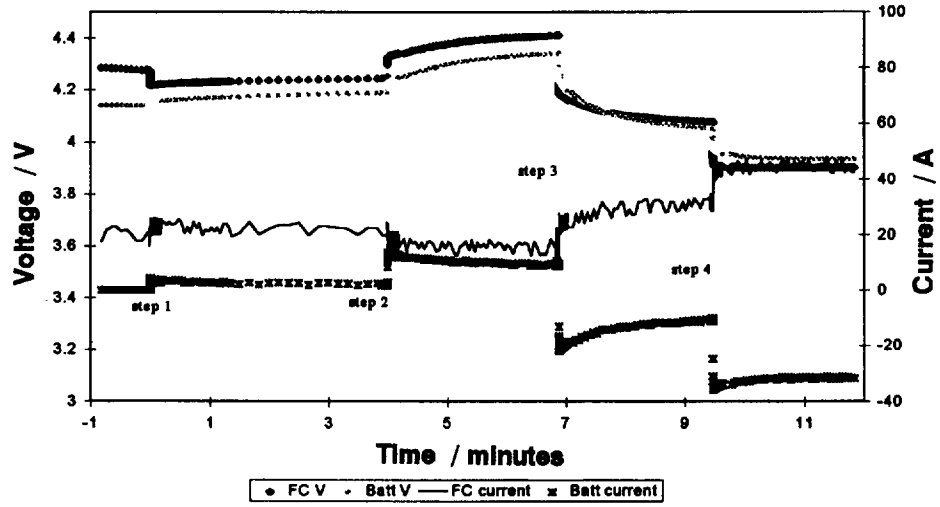

Fig. 6. Response of the coupled battery and fuel cell. Step 1: battery connected to the discharging fuel cell. Step 2: load removed from the bus. Step 3: load added to bus. Step 4: a second load added to the bus.

state voltage between the systems as shown in Fig. 6. As expected, the fuel cell voltage did not overshoot when coupled with the battery.

When a load was dropped, the system response time was considerably shorter than that of the battery alone, with steady state being reached in the order of a few minutes. The difference between the battery and fuel cell voltages was caused by shunt resistances between the units. When a load was then added to the system, both sources provided power, with a large percentage of the current coming from the battery until the battery voltage had time to fall. Adding another load had a much smaller impact, as the battery voltage had already shifted, and the battery's non-ohmic resistance term, R_2, decreased with increasing voltage.

Altering the battery characteristics by the addition of a second parallel string of battery cells resulted in very similar behaviour, except that the system moved more quickly to steady state and there was less voltage movement.

The system behaviour was accurately predicted by the model (Fig. 7), but the results indicated that the system established when the fuel cell was coupled to a single battery branch showed a slightly larger capacitive effect than anticipated. This discrepancy disappeared in the scenario with the second battery branch. The model also predicted that a slightly larger fraction of the current would be provided by the battery than was observed after step 4. This can be alleviated by improving the estimate of the R_2 battery term at higher discharge currents (the current flowing in the battery

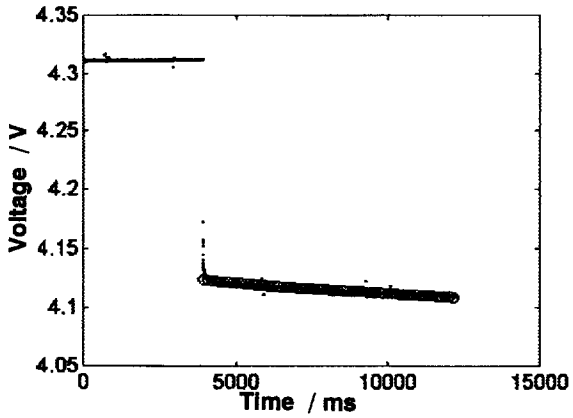

Fig. 7. Comparison of experimental voltage drop across load (dots) with predictions from the model (circles). Drop occurring at the same time as step 3 in Fig. 6.

after step 4 was at a $C/8$ rate, which was higher than the initial correlation). Further investigations also indicated that in the two-battery system, the fuel cell capacitance term adds extremely little to the simulation and can be eliminated from the model.

4.4. Scale-up

A Canadian Oberon submarine battery has 224 lead–acid cells in series, all of which have an extremely low internal resistance. When this is scaled up, a number of observations are noteworthy. First, the large number of lead–acid cells will result in a significant decrease in the battery capacitance, while the battery resistance remains relatively small (it has to be small to prevent overheating). Similarly, since there will be hundreds of fuel cells in series, the fuel cell capacitance will not be visible. Secondly, when paralleled with a 400 kW fuel cell system, the ratio of the resistance of the fuel cell stack to the battery resistance will change with changing battery SOC and current density. The ratio will be of the order of 1/1 to 5/1, depending on the current density. This could result in the battery supplying a much larger percentage of the current when higher loads are present.

Two scenarios are worth mentioning. First, the battery will act as an instantaneous power source if the fuel cell was unable to instantly respond to a load change. The battery will likely provide the majority of the power at high loads. However, at all times, when within the power envelope of the fuel cell stack, it would be desirable to maximise the power being supplied by the fuel cell. For this reason, the fuel cell's control strategy will have to be designed to ensure that this is the case.

The second scenario involves the system behaviour in response to a sudden load shed. If the battery was at over 80% SOC, there still exists the risk that the sudden current flowing to the battery could cause excessive levels of hydrogen production. However, the buffering of the system predicted by the model and demonstrated by bench testing suggest that this will not be a problem if a control system is in place and float charging the batteries while underwater is permissible.

5. Conclusions

Representing a hybrid fuel cell/battery system as an electric circuit is a useful tool for evaluating how the systems will interact. It will also permit a straightforward approach to investigating different series/parallel combinations of fuel cells and batteries. However, the very simplicity of the model implies that there will be slight errors in estimating the battery voltage during charging.

References

[1] Z.M. Salameh, M.A. Casacca and W.A. Lynch, *IEEE Trans. Energy Conversion*, 7 (1) (1992) 93–97.
[2] S.A. Ilangovan, *J. Power Sources*, 50 (1994) 33–45.
[3] J.C. Amphlett, R.M. Baumert, R.F. Mann, B.A. Peppley, P.R. Roberge and T.J. Harris, *J. Electrochem. Soc.*, 142 (1) (1995) 1–8.
[4] J.C. Amphlett, R.M. Baumert, R.F. Mann, B.A. Peppley, P.R. Roberge and T.J. Harris, *J. Electrochem. Soc.*, 142 (1) (1995) 9–15.
[5] J.C. Amphlett, R.M. Baumert, R.F. Mann, B.A. Peppley, P.R. Roberge and A. Rodrigues, *J. Power Sources*, 49 (1994) 349–356.
[6] R. Baumert and D. Epp, *Proc. Oceans '93 Conf., Victoria, BC, Oct. 1993*, Vol. 2.